



High-energy spectrum and zenith-angle distribution of atmospheric neutrinos

S. I. SINEGOVSKY¹, O. N. PETROVA¹, T. S. SINEGOVSKAYA²

¹*Irkutsk State University, Irkutsk, 664003, Russia*

²*Irkutsk State Railway University, Irkutsk, 664046, Russia*
 sinegovsky@api.isu.ru

Abstract: High-energy neutrinos, arising from decays of mesons produced through the collisions of cosmic ray particles with air nuclei, form the background in the astrophysical neutrino detection problem. An ambiguity in high-energy behavior of pion and especially kaon production cross sections for nucleon-nucleus collisions may affect essentially the calculated neutrino flux. We present results of the calculation of the energy spectrum and zenith-angle distribution of the muon and electron atmospheric neutrinos in the energy range 10 GeV to 10 PeV. The calculation was performed with usage of known hadronic models (QGSJET-II, SIBYLL 2.1, Kimel & Mokhov) for two of the primary spectrum parametrizations, by Gaisser & Honda and by Zatsepin & Sokolskaya. The comparison of zenith angle-averaged muon neutrino spectrum with the measurement data in IceCube experiment make it clear that even at energies above 100 TeV the prompt neutrino contribution is not so apparent because of tangled uncertainties of the strange (kaons) and charm (*D*-mesons) particle production cross sections. An analytic description of calculated neutrino fluxes is presented.

Keywords: atmospheric neutrinos, high-energy hadronic interactions

1 Introduction

Atmospheric neutrinos (AN) appear in decays of mesons (charged pions, kaons etc.) produced through collisions of high-energy cosmic rays with air nuclei. The AN flux in the wide energy range remains the issue of the interest since the low energy AN flux is a research matter in the neutrino oscillations studies, and the high energy atmospheric neutrino flux is now appearing as the background noise for astrophysical neutrino experiments [1, 2, 3, 4, 5, 6, 7].

In spite of numerous AN flux calculations are made (for example [8, 9, 10, 11, 12, 13, 14, 15], see also [16, 17] for a review of 1D and 3D calculations of the AN flux) there are questions concerning to the flux uncertainties originated from hadronic interaction models as well as from uncertainties in primary cosmic ray spectra and composition in the “knee” region.

In this work we present results of the atmospheric neutrino flux calculation in the range $10-10^7$ GeV made with use of the hadronic models QGSJET-II 03 [18], SIBYLL 2.1 [19] as well as the model by Kimel & Mokhov (KM) [20] that were tested also in recent atmospheric muon flux calculations [21, 22]. We compute here the differential energy spectrum of the conventional neutrinos averaged over zenith angles to compare with the data of the Frejus [1], AMANDA-II [4] and IceCube [5] experiments.

2 Calculations vs. the experiment

The calculation is performed on the basis of the method [23] of solution of the hadronic cascade equations in the atmosphere, which takes into account non-scaling behavior of inclusive particle production cross-sections, the rise of total inelastic hadron-nuclei cross-sections, and the non-power law primary spectrum (see also [15, 21, 22]). Along with major sources of the muon neutrinos, $\pi_{\mu 2}$ and $K_{\mu 2}$ decays, we consider three-particle semileptonic decays, $K_{\mu 3}^{\pm}$, $K_{\mu 3}^0$, the contribution originated from decay chains $\bar{K} \rightarrow \pi \rightarrow \nu_{\mu}$ ($K_S^0 \rightarrow \pi^+ \pi^-$, $K^{\pm} \rightarrow \pi^{\pm} \pi^0$), as well as small fraction from the muon decays. One can neglect the 3D effects in calculations of the atmospheric muon neutrino flux near vertical at energies $E \gtrsim 1$ GeV and at $E \gtrsim 5$ GeV in case of directions close to horizontal (see [13, 14]). As the primary cosmic ray spectra and composition in wide energy range we use the model recently proposed by Zatsepin & Sokolskaya (ZS) [24], which fits well the ATIC-2 experiment data [25] and supposedly to be valid up to 100 PeV. The ZS proton spectrum at $E \gtrsim 10^6$ GeV is compatible with KASCADE data [26] as well the helium one within the range of the KASCADE spectrum obtained with the usage of QGSJET 01 and SIBYLL models. Alternatively in the energy range $10-10^6$ GeV we use the parameterization by Gaisser, Honda, Lipari and Stanev (GH) [17], the version with the high fit to the helium data. Note this version is consistent with the data of the KAS-

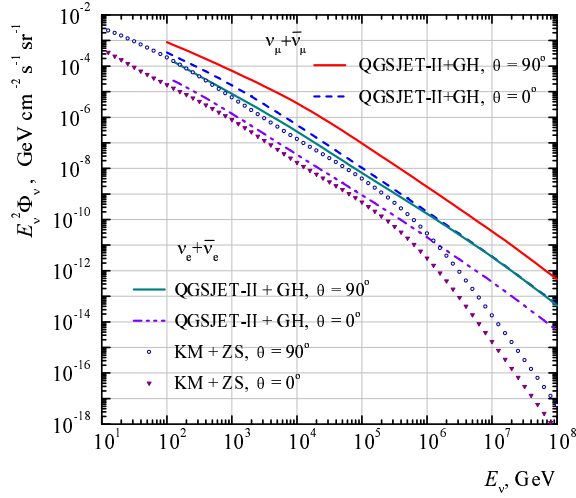


Figure 1: Spectra of the conventional muon and electron neutrinos calculated for vertical and horizontal directions.

CADE experiment at $E_0 > 10^6$ GeV that was obtained (through the EAS simulations) with the SIBYLL 2.1.

Figures 1, 2 display the scale of difference between the conventional $(\nu_{\mu} + \bar{\nu}_{\mu})$ spectra and $(\nu_e + \bar{\nu}_e)$ one, calculated with usage of QGSJET-II, SIBYLL and KM model for GH and ZS primary spectra. The difference of neutrino flux predictions related to choice of hadronic models is clearly apparent.

Zenith-angle distributions of the conventional neutrinos, $\phi_{\nu_{\mu}}(E, \theta)/\phi_{\nu_{\mu}}(E, 0^\circ)$, for the energy range 1-10⁵ TeV are shown in Fig. 3. Calculations are made with QGSJET-II and SIBYLL 2.1 models both for GH and ZS (ATIC-2) primary spectra and composition. As was expected, a shape of the angle distribution visibly depends on the neutrino energy (at $E < 100$ TeV) especially for directions close to horizontal. The effect of the hadronic models (as well as

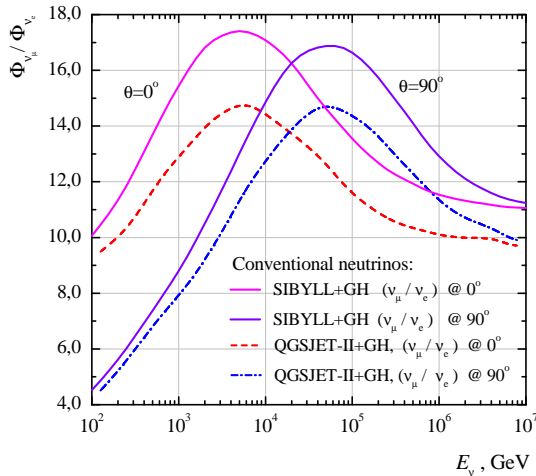


Figure 2: Conventional neutrino flavor ratios calculated with SIBYLL and QGSJET-II hadronic models for the GH primary spectrum.

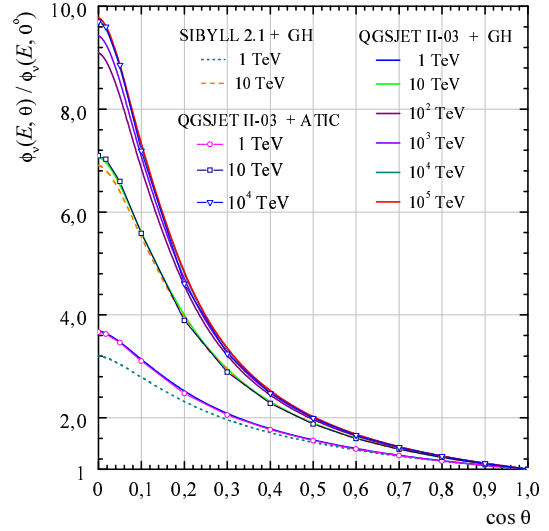


Figure 3: Zenith-angle enhancement of the $(\nu_{\mu} + \bar{\nu}_{\mu})$ flux.

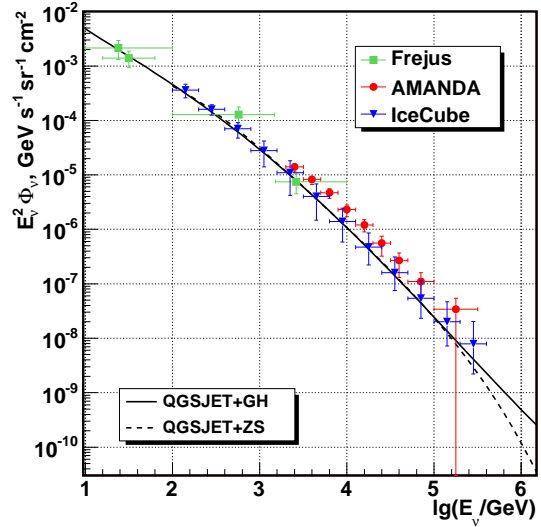


Figure 4: Conventional $(\nu_{\mu} + \bar{\nu}_{\mu})$ spectrum averaged over zenith angles. Curves: the calculation with usage of QGSJET-II. Symbols: data of experiments, Frejus [1], AMANDA-II [4], IceCube [5].

of the primary spectrum) on the angle distribution is rather weak, while the spectra differences amount to 80% [15].

The calculation of the conventional $(\nu_{\mu} + \bar{\nu}_{\mu})$ flux averaged over zenith angles as compared with Frejus [1] (squares), AMANDA-II [4] (circles), and IceCube [5] (triangles) measurement data is shown in Figs. 4, 5. Figure 4 displays the conventional $(\nu_{\mu} + \bar{\nu}_{\mu})$ spectrum (averaged over zenith angles in the range $0^\circ - 84^\circ$) calculated with usage of QGSJET-II model for GH primary spectra and composition (solid line) as well as for ZS one (dashed). The difference in neutrino flux predictions resulted from the primary cosmic ray spectra becomes apparent at high neutrino energies: the flux obtained with QGSJET-II for GH

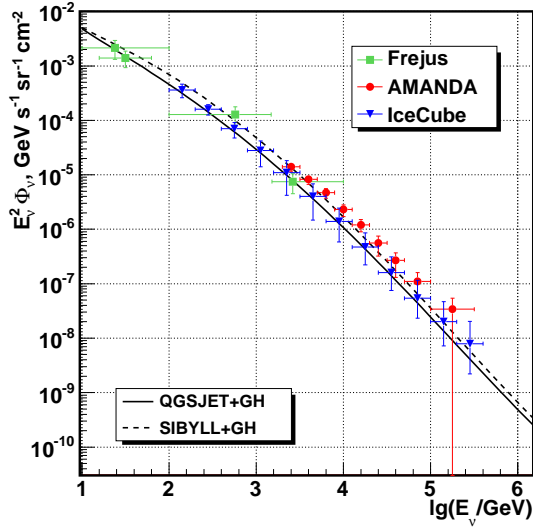


Figure 5: Comparison of the $(\nu_\mu + \bar{\nu}_\mu)$ spectrum calculations with QGSJET-II and SIBYLL 2.1

spectrum at 600 TeV is nearly twice as large as that for ZS spectrum. At 1 PeV this discrepancy increases to the factor about five. Comparison of QGSJET-II and SIBYLL presented in Fig. 5 shows that the former seems more preferable to describe the IceCube measurements at the energies below 40 TeV (conventional neutrinos).

The usage of QGSJET-II and SIBYLL models leads to apparent difference in the neutrino flux, as well as in the case of SIBYLL as compared to KM (unlike the muon flux, where SIBYLL and KM lead to very similar results [21]). On the contrary, the QGSJET-II neutrino flux is very close to the KM one: up to 100 TeV the difference does not exceed 5% for the GH spectrum and 10% for the ZS one at $\theta = 0^\circ$. Note that the muon flux discrepancy in QGSJET-II and KM predictions is about 30% at vertical [21].

Figure 6 shows the sum of the conventional flux (calculated for GH spectrum with usage of QGSJET-II) and prompt muon neutrino flux predictions [27] (see also [11, 16, 28]) due to nonperturbative models, the recombination quark-parton model (RQPM, dotted line) and the quark-gluon string model (QGSM, dashed line). The case of ZS spectrum one can see in Fig. 7. The prompt neutrino fluxes were obtained [27] with NSU primary spectrum [29], therefore they can serve here as upper limits for the prompt neutrino flux due to RQPM and QGSM. It worth noting that evaluation of the prompt neutrino flux obtained with the dipole model [30] is close to the QGSM prediction [27] above 1 PeV. The prompt neutrino flux due to QGSM in the energy range $5 \text{ TeV} \leq E_\nu \leq 5 \cdot 10^3 \text{ TeV}$ was approximated by the expression

$$\Phi_\nu^{\text{pr}}(E_\nu) = A(E_1/E_\nu)^{3.01} [1 + (E_1/E_\nu)^{2.01}]^{-0.165}, \quad (1)$$

where $A = 1.19 \cdot 10^{-18} (\text{GeV cm}^2 \text{ s sr})^{-1}$, $E_1 = 100 \text{ TeV}$. In this range we neglect the weak angle dependence of the prompt neutrino flux.

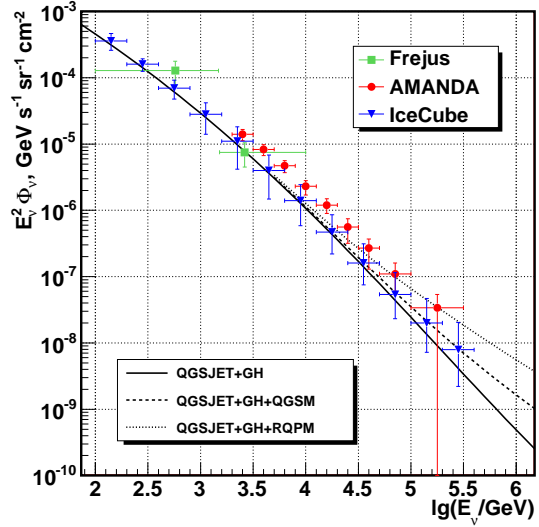


Figure 6: Flux of the conventional and prompt muon neutrinos (case of GH spectrum).

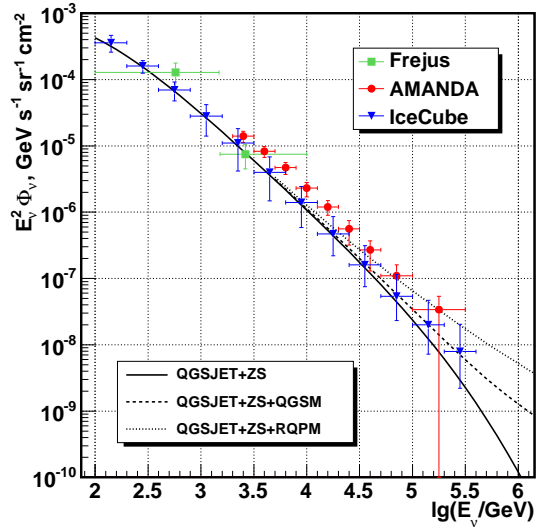


Figure 7: Flux of the conventional and prompt muon neutrinos (case of QGSJET-II + ZS spectrum).

3 Approximation formula

Numerical results of the conventional muon neutrino spectra in the energy range $10^2 - 10^6 \text{ GeV}$ for different zenith angles can be approximated with accuracy $(3 \div 8)\%$ by the formula:

$$\log_{10}[E_\nu^2 \Phi_\nu(E_\nu, \theta)] = \sum_{k=0}^4 \sum_{n=0}^3 a_{kn} x^n y^k. \quad (2)$$

Here $\Phi_\nu(E_\nu, \theta)$ is the flux with units of $\text{GeV}^{-1} \text{ s}^{-1} \text{ sr}^{-1} \text{ cm}^{-2}$, $x = \cos \theta$, $y = \log_{10}(E_\nu/\text{GeV})$. Coefficients a_{kn} are given in Tables 1, 2.

Table 1: Coefficients a_{kn} for the QGSJET+GH choice

k	n			
	0	1	2	3
	a_{kn}			
0	0.72550	-6.45625	4.10284	-0.87026
1	-3.21166	6.38522	-3.31293	0.38300
2	1.00337	-2.46611	0.99745	0.01675
3	-0.19397	0.35758	-0.07515	-0.04540
4	0.01211	-0.01753	-0.00135	0.00537

Table 2: Coefficients a_{kn} for the QGSJET+ZS choice

k	n			
	0	1	2	3
	a_{kn}			
0	-3.21881	-7.00088	4.64475	-1.07882
1	1.60632	6.92858	-3.87209	0.60250
2	-1.11835	-2.65863	1.20056	-0.06412
3	0.20848	0.38659	-0.10641	-0.03279
4	-0.01577	-0.01909	0.00037	0.00467

4 Summary

The calculations of the high-energy atmospheric muon neutrino flux demonstrate rather weak dependence on the primary spectrum models in the energy range $10-10^5$ GeV. However the picture appears less steady because of sizable flux differences originated from the models of high-energy hadronic interactions. As it can be seen by the example of the models QGSJET-II and SIBYLL 2.1, the major factor of the discrepancy in the conventional neutrino flux is the kaon production in nucleon-nucleus collisions.

Comparison of calculated muon neutrino flux with the spectrum measured by IceCube shows that QGSJET-II is preferable model irrespective of the primary spectrum choice. The prompt neutrino contribution due to quark gluon string model (QGSM) added to the conventional one lead to better agreement with the IceCube measurement above 100 TeV.

The work was supported by Russian Federation Ministry of Education and Science within the Federal Programs "Scientific and educational specialists for innovative Russia" under Contracts 14.740.11.0890, P681, P1242, and "Development of scientific potential in Higher Schools" under grant 2.2.1.1/12360.

References

- [1] K. Daum et al. (Frejus Collaboration), *Z. Phys. C*, 1995, **66**, 417-428.
- [2] A. Avrorin et al. *Nucl. Instrum. Meth. A*, 2011, **626-627**, S13.
- [3] V.M. Aynutdinov et al. *Russ. Phys. J.* 2010, **53**, 601-610.
- [4] R. Abbasi et al. (IceCube Collaboration), *Astropart. Phys.* 2010, **34**, 48-58.
- [5] R. Abbasi et al. (IceCube Collaboration), *Phys. Rev. D*, 2011, **83**, 012001.
- [6] T. Montaruli, for the IceCube Collaboration, *Nucl. Phys. B (Proc. Suppl.)* 2011, **212-213**, 99-108.
- [7] S. Biagi, for the ANTARES Collaboration, *Nucl. Phys. B (Proc. Suppl.)* 2011, **212-213**, 109-114; A. Margiotta et al. *Nucl. Phys. B (Proc. Suppl.)* 2009, **190**, 121-126.
- [8] L.V. Volkova, *Sov. J. Nucl. Phys.* 1980, **31**, 784-790.
- [9] A.V. Butkevich, L.G. Dedenko, I.M. Zheleznykh, *Sov. J. Nucl. Phys.* 1989, **50**, 90-99.
- [10] P. Lipari, *Astropart. Phys.* 1993, **1**, 195-227.
- [11] V.A. Naumov, T.S. Sinegovskaya, S.I. Sinegovsky, *Il Nuovo Cim. A*, 1998, **111**, 129-147.
- [12] G. Fiorentini, V.A. Naumov, F.L. Villante, *Phys. Lett. B*, 2001, **510**, 173-188.
- [13] G.D. Barr et al. *Phys. Rev. D*, 2004, **70**, 023006.
- [14] M. Honda et al. *Phys. Rev. D*, 2004, **70**, 043008.
- [15] A.A. Kochanov, T.S. Sinegovskaya, S.I. Sinegovsky, arXiv:0906.0671v2; S.I. Sinegovsky, A.A. Kochanov, T.S. Sinegovskaya, arXiv:1010.2336v1.
- [16] V.A. Naumov, hep-ph/0201310.
- [17] T.K. Gaisser, M. Honda, *Annu. Rev. Nucl. Part. Sci.* 2002, **52**, 153-199.
- [18] S.S. Ostapchenko, *Nucl. Phys. B (Proc. Suppl.)* 2006, **151**, 143-146; S. Ostapchenko, *Phys. Rev. D*, 2006, **74**, 014026.
- [19] R.S. Fletcher et al. *Phys. Rev. D*, 1994, **50**, 5710-5731; E.-J. Ahn et al. *Phys. Rev. D*, 2009, **80**, 094003.
- [20] A.N. Kalinovsky, N.V. Mokhov, Yu.P. Nikitin, 1989. Passage of high-energy particles through matter, New York, USA: AIP (1989) 262 p.
- [21] A.A. Kochanov, T.S. Sinegovskaya, S.I. Sinegovsky, *Astropart. Phys.* 2008, **30**, 219-233.
- [22] S.I. Sinegovsky et al. *Int. J. Mod. Phys. A*, 2010, **25**, 3733-3740; arXiv:0906.3791.
- [23] V.A. Naumov, T.S. Sinegovskaya, *Phys. Atom. Nucl.* 2000, **63**, 1927-1935.
- [24] V.I. Zatsepin, N.V. Sokolskaya, *Astronomy & Astrophys.* 2006, **458**, 1-5; *Astron. Lett.* 2007, **33**, 25-33.
- [25] A.D. Panov et al., *Bull. Russ. Acad. Sci. Phys.* 2007, **71**, 494-497; astro-ph/0612377.
- [26] T. Antoni et al., *Astropart. Phys.* 2005, **24**, 1-25; W.D. Apel et al. *Astropart. Phys.* 2009, **31**, 86-91.
- [27] E.V. Bugaev et al. *Nuovo Cim. C*, 1989, **12**, 41-73.
- [28] E.V. Bugaev et al. *Phys. Rev. D*, 1998, **58**, 054001.
- [29] S.I. Nikolsky, I.N. Stamenov, S.Z. Ushev, *Sov. Phys. JETP*, 1984, **60**, 10-21.
- [30] R. Enberg, M.H. Reno, I. Sarcevic, *Phys. Rev. D*, 2008, **78**, 043005.